Supporting Information

Coral-like porous tubular Ni doped g-C_3N_4 nanocomposites as bifunctional templates for photocatalytic degradation and fluorescence detection of sunset yellow in beverages

Yue Li[a], Ping Liu[b], Shisen Li[a], Yanting Ren[b], Wenzhen Du[a], Wenjing Yin[b], Haiyan Jiang[a], Qingli Yang[b], Yongchao Ma[a,] *

[a] College of Chemistry and Pharmaceutical Sciences, Qingdao Agricultural University, Qingdao, 266109, P. R. China

[b] College of Food Science and Engineering, Qingdao Agricultural University, Qingdao, 266109, P. R. China

*Corresponding authors: yongchaoma@126.com.

Characterization

The microscopic morphology of the produced catalysts was examined using field emission scanning electron microscopy (SEM, S-4800, Hitachi) and field-emission transmission electron microscopy (TEM, JOEL JEM 2001). The structures were analyzed by X-ray powder diffractometry (XRD, TD-3700, China) and Fourier transform infrared spectroscopy (FTIR, Nicolet iS10, USA). The pore size distribution was assessed using the Barrett-Joyner-Halenda (BJH) method on a Quantatech N22-27E analyzer. The valence states of the elements were examined using X-ray photoelectron spectroscopy (XPS, Thermo Escalab 250Xi, USA). The light absorption characteristics were assessed using an ultraviolet-visible spectrometer equipped with an integrating sphere (UV–vis DRS, Shimadzu UV-3900, Japan). Photo-luminescence (PL) spectroscopy was conducted using a fluorescence spectrometer (PL, Shimadzu F-7000, Japan). Time-resolved fluorescence spectroscopy (TRPL) was evaluated using the FLS1000 from Edinburgh Instruments, UK.

For the photoelectrochemical experiments, an Ag/AgCl electrode was selected as the reference electrode, while a Pt sheet electrode served as the counter electrode. The experiments were conducted using an electrochemical workstation (CHI660E, Chenhua, Shanghai, China) using a 0.1 M Na_2SO_4 solution as the electrolyte. A 300 W xenon lamp was chosen as the light source, and the transient photocurrent response with a bias voltage of -0.27 V was evaluated over time throughout the on/off illumination cycle. The electrochemical impedance spectra were recorded throughout a frequency range of 1000 kHz to 0.01 Hz, while the Mott-Schottky curves were evaluated within a voltage range of -1 to 1 V.

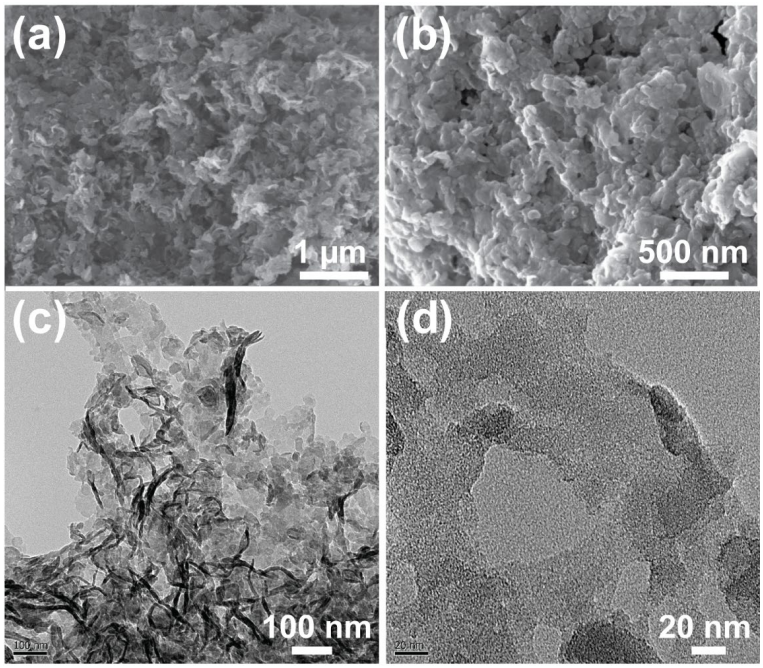

Fig. S1. (a, b) SEM and (c, d) TEM images with different magnifications of pristine CN samples.

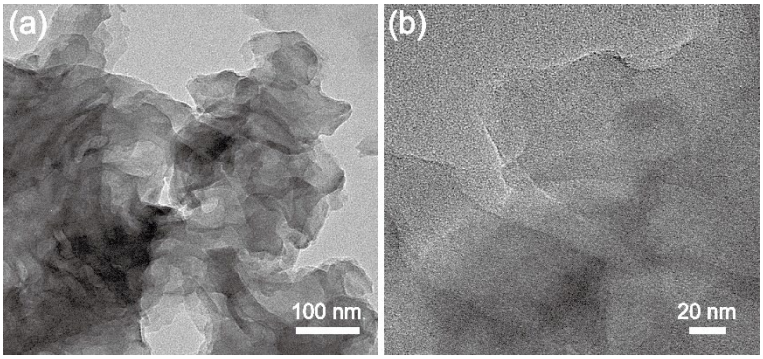

Fig. S2. (a, b) TEM images with different magnifications of Ni-CN NS.

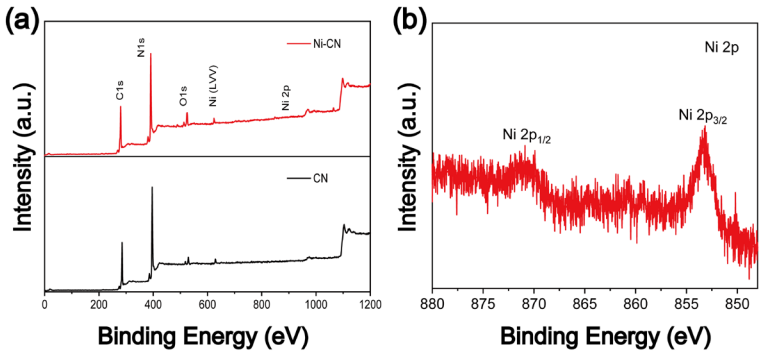

Fig. S3. (a) XPS survey spectra of CN and Ni-CN-0.5 samples. (b) high-resolution spectra of Ni-CN-0.5 sample.

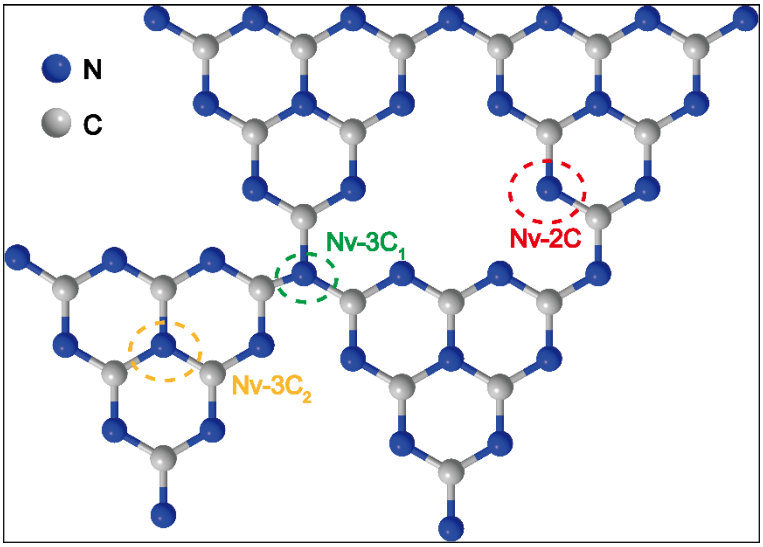

Fig. S4. The schematic diagram of three different N vacancies in carbon nitride: Nv-2C, Nv-$3C_1$, and Nv-$3C_2$.

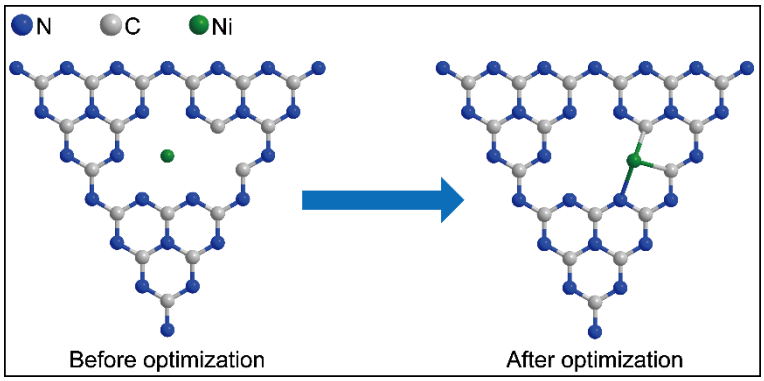

Fig. S5. Initial and optimized coordination structures of Ni single atoms on g-C_3N_4 structural units.

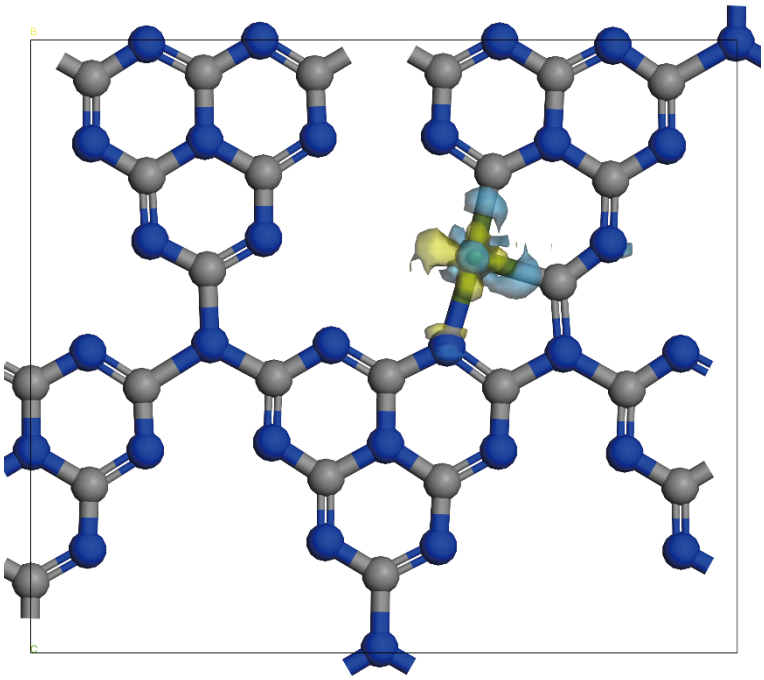

Fig. S6. Charge density differences for Ni-CN-0.5, in which yellow and light blue represent electron accumulation and depletion, respectively (Green: Ni single atom. Blue: N atoms. Grey: C atoms).

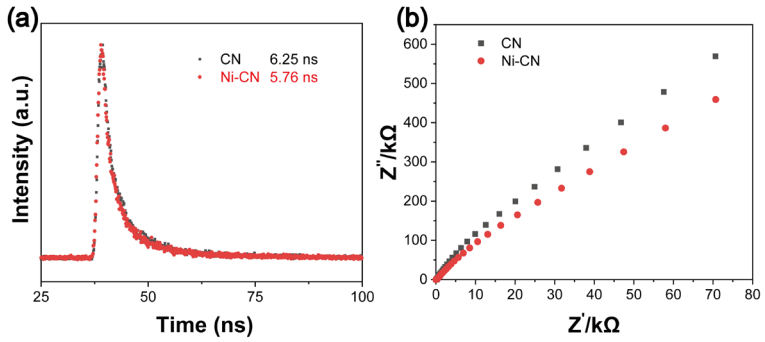

Fig. S7. (a) TRPL spectra and (b) EIS Nyquist plots of CN and Ni-CN-0.5.

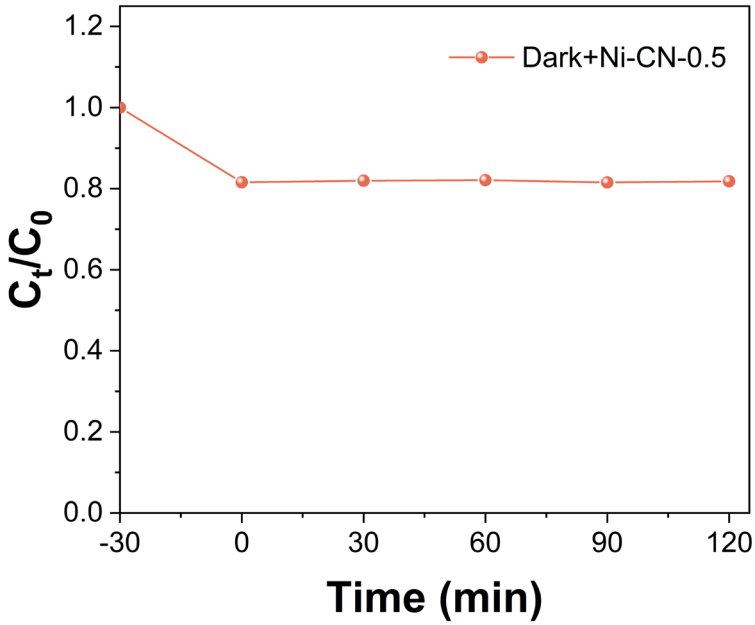

Fig. S8. *Photocatalytic degradation curves of Ni-CN-0.5 sample for SY under dark conditions*

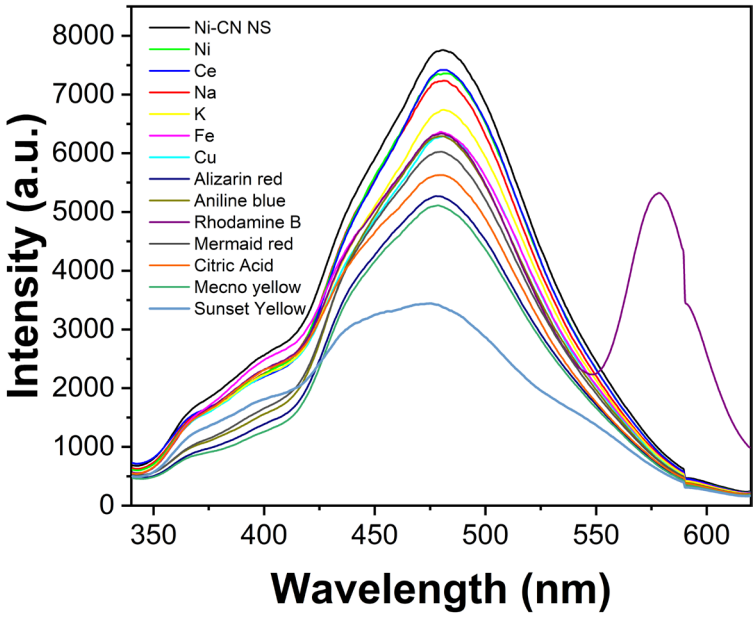

Fig. S9*. Changes in fluorescence emission of Ni-CN NS on the addition of various analytes.*

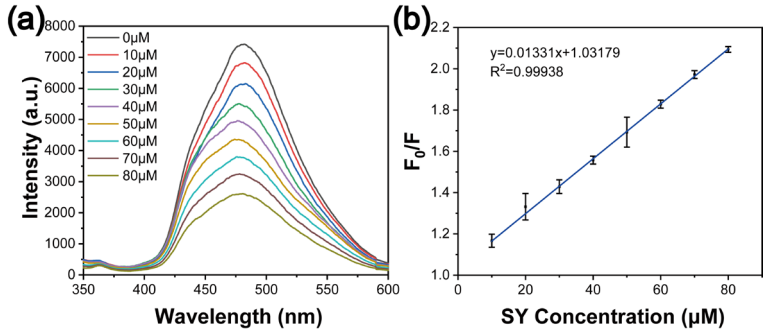

Fig. S10. (a) Changes in the emission spectra of Ni-CN NS for orange juice in the presence of SY.

(b) Linearity of F_0/F versus SY concentration in orange juice (10.0-80.0 μM).

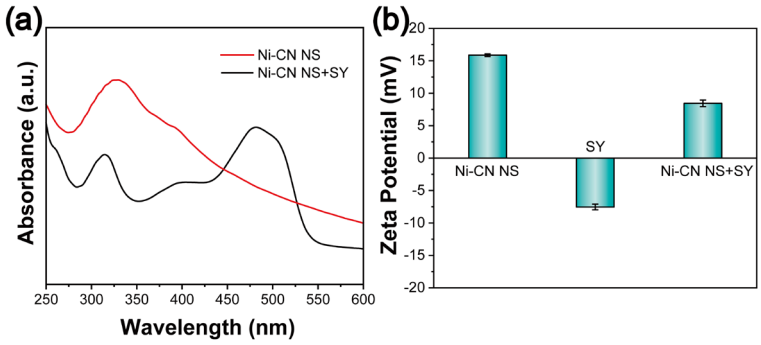

Fig. S11. (a)Absorption spectra of Ni-CN NS before and after the addition of SY, (b) Ni-CN NS before and after the addition of SY and the zeta potential of SY.

Table S1. Fluorescence decay results of CN and Ni-CN.

Sample	τ_1/ns	B_1(%)	τ_2/ns	B_2(%)	Average/ns
CN	2.2784	46.02	9.6423	53.98	6.25
Ni-CN	2.1516	47.98	9.0808	52.02	5.76

Table S2 Detection of SY in a real sample (n = 3)

Sample	Spiked (μM)	Found (μM)	Recovery (%)	RSD (%, n=3)
Orange juice	10	9.48	94.8	1.49
	20	19.76	98.8	2.74
	30	29.57	98.57	1.15

The above results are the average of three repeated experiments.

Table S3. fluorescence decay results of Ni-CN NS after the addition of SY.

Sample	τ_1/ns	B_1(%)	τ_2/ns	B_2(%)	τ_3/ns	B_3(%)	Average/ns
Ni-CN NS	0.7904	18.86	3.5436	53.63	12.9204	27.51	5.6
Ni-CN NS+SY	0.5658	28.01	2.6891	51.46	11.4343	20.53	3.89

Table S4. Comparison with other photocatalysts for LY or other analogs degradation.

Photocatalyst	Light source	Sunset Yellow Removal(%)	C_0/mg/L	Dosage (g/L)	Time (min)	Reference
CS–ZnSe	solar radiation	97%	20-30	1	180	[1]
rGO-CdS	4150 lumens 85 W Oreva CFL bulb (450 < λ < 650 nm)	66%	10	0.5	270	[2]
ZnCo-LDHs/g-C_3N_4	UV irradiation (λ = 365 nm)	99.6%	75	1.25	90	[3]
Se-NPLs	solar radiation	83.8%	5	0.3	600	[4]
CDCNs	300 W Xenon lamp ultraviolet cut-off and an infrared filter (420 < λ < 780 nm)	96.3%	2.5	0.11	60	[5]
PMS-driven CFO	150 W four visible Osram lamps (400 < λ < 800 nm)	91.8%	14.02	0.49	120	[6]
Ni-CN	300 W xenon lamp cut-off filter (λ = 420 nm)	96.9%	10	0.3	120	Our work

References

1. S. Zhang, Saeeda, A. Khan, N. Ali, S. Malik, H. Khan, N. Ali, H. M. N. Iqbal and M. Bilal, *Environ Res*, 2022, **213**, 113722.
2. M. Kaur, A. Umar, S. K. Mehta and S. K. Kansal, *Applied Catalysis B: Environmental*, 2019, **245**, 143-158.
3. Z. Jie, L. Yang, T. Huiyuan, X. Mengyan, D. Xiuhong, W. Zehua, L. Chunguang, D. Xianying and C. Jiehu, *Environ Sci Pollut Res Int*, 2023, **30**, 100450-100465.
4. R. Hassanien, A. A. I. Abed-Elmageed and D. Z. Husein, *ChemistrySelect*, 2019, **4**, 9018-9026.
5. D. Gong, J. Guo, F. Wang, J. Zhang, S. Song, B. Feng, X. Zhang and W. Zhang, *Food Chem*, 2023, **425**, 136470.
6. Ö. Tuna and E. Bilgin Simsek, *Optical Materials*, 2023, **142**.